

Characterization of Bamboo-Derived Cellulose Via Combined Pretreatment and Dissolution Effect in Ionic Liquid

Loi Xue Min¹, Mazatusziha Ahmad^{2*}, Mohammad Nazrul Roslan^{3*}

¹Department of Chemical Engineering Technology, Faculty of Engineering Technology,
Universiti Tun Hussein Onn Malaysia, 84600 Pagoh, Johor, MALAYSIA

²Bamboo Research Centre, Faculty of Engineering Technology, Universiti Tun Hussein Onn Malaysia, Pagoh Higher Education Hub, 84600 Pagoh, Johor, MALAYSIA

³Department of Mechanical Engineering Technology, Faculty of Engineering Technology,
Universiti Tun Hussein Onn Malaysia, 84600 Pagoh, Johor, MALAYSIA

*Corresponding Author Designation

DOI: <https://doi.org/10.30880/peat.2023.04.02.102>

Received 15 January 2023; Accepted 12 February 2023; Available online 12 February 2023

Abstract: Recently, ionic liquid (ILs) as a green solvent has replaced the use of volatile organic solvent in the dissolution of cellulose for bio-based fabrics. This study aims to characterize the bamboo-derived cellulose and dissolution effects of cellulose in two types of ionic liquids; 1-allyl-3-methyl-imidazolium-chloride, [AMIM]Cl and 1-butyl-3-methyl-imidazolium chloride, [BMIM]Cl prior formation of regenerated cellulose film. The film was synthesized using cellulose extracted from bamboo, *Schizostachyum grande* via a combination of mechanical and chemical pre-treatment. The extracted bamboo was characterized using particle size analyser (PSA), Fourier-transform infrared spectroscopy (FTIR), X-ray Diffraction (XRD), Differential Scanning Calorimetry (DSC) and Thermal Gravimetric Analysis (TGA). Comparisons were made between the extracted bamboo with raw bamboo fiber and commercial microcrystalline cellulose (MCC). The extracted cellulose was confirmed by removal of lignin. The disappearance of FTIR spectra at 1722 cm^{-1} and 1602.8 cm^{-1} which correspond to the C=O stretching frequency of ester group and the stretching vibration of aromatic rings, respectively indicates the removal of lignin. The XRD results showed a significant reduction of crystallinity index (CrI %) in RBF as compared to bamboo cellulose (BC) due to removal of amorphous regions during the chemical treatment. The DSC analysis further confirmed the reduction of crystalline regions in cellulose extracted from bamboo. Similarly, the dissolution and

regeneration process reduced the crystallinity of cellulose. However, the dissolution in ionic liquids failed to form a film. Overall, it can be concluded that the absence of co-solvent, inefficient heating approach as well as the degradation of cellulose during dissolution possibly act as contribution factors upon the film formation.

Keywords: Ionic Liquid, Bamboo Cellulose, Cellulose Dissolution, Regenerated Film, Characterization

1. Introduction

Considerable attention has been paid to cellulose as a biopolymer due to its superior mechanical properties, in terms of tensile and flexural strengths, modulus as well as good heat resistance [1]. Cellulose is one of the major elements in the plant cell walls that provides structural support. The cellulose extracted from plant fiber potentially acts as a versatile resource of regenerated cellulose for textile applications as it provides soft, breathable and has anti-microbial and UV protection properties, which makes it a unique eco-friendly textile in the 21st century as compared to synthetic cellulosic fibers. Cellulose commonly undergoes a combined method of pre-treatment whereas after the cellulose is extracted, it will be further dissolved in an organic solvent for better surface modification. After numerous methods of extraction are introduced such as mechanically, chemically or biologically, dissolution of lignocellulosic biomass often led to difficulties with the use of conventional organic solvent. However, conventional organic solvents are often corrosive and highly volatile, in which certain temperature or pressure will affect the concentration and make it easy to vaporize within the air.

Currently, there are two industrially established technologies for the manufacture of synthetic cellulosic fibers which are the viscose and Lyocell processes. Nevertheless, they revealed that the problems occurred related to the highly toxic chemicals that were used as solvents during the cellulose dissolution stage. The N-methyl morpholine-N-oxide (NNMO monohydrate) is presently used as the solvent in the Lyocell process and has numerous drawbacks which led to environmental pollution. These include serious solvent recovery procedures, complex dissolution techniques, the poor thermal stability of NNMO, low productivity as a result of cellulose's poor solubility in NNMO and high safety expenses.

Dissolution of cellulosic biomass often led to difficulties with the use of conventional organic solvents. The presence of strong inter-and intra- molecular hydrogen bonds makes cellulose insoluble in water and most organic solvents results in limited reactivity and processability. In addition, these conventional approaches may cause high volatility, in which certain temperatures or pressure will affect the concentration and make it easy to vaporize within the air, and even harmful to the environment. Therefore, the usage of a greener approach is desired to eliminate and minimize environmental problems. Ionic liquids (ILs) have been suggested as solvents for the dissolution of cellulose. It has the ability to dissolve cellulose in high concentrations, around 15-20%. IL have various benefits over conventional solvents due to their ionic structure, including the lack of observable and quantifiable vapour pressure, simplicity of recycling, excellent chemical compound dissolving properties, and great thermal stability. Thus, in this study, the dissolution effects of extracted bamboo cellulose in ionic liquids, 1-allyl-3-methyl-imidazolium-chloride, [AMIM]Cl and 1-butyl-3-methyl-imidazolium chloride, [BMIM]Cl were studied and investigated.

2. Materials and Methods

The bamboo, *Schizostachyum grande* was processed into long fiber using fiber a extraction machine before grinded into powder using a planetary ball mill to obtain raw bamboo fiber (RBF) After that, the

sample was sieved with a 75 μ m mesh size sieve. The bamboo fiber was dewaxed using the Leavitt-Danzer method using a Soxhlet reactor. The extraction process was approximately 2 hours with 10-12 cycles of extraction until the mixture colour disappeared. The product (DBF) was washed and filtered before being dried in an oven at 70°C overnight.

DBF was then immersed into a delignification solution prepared using 82.3g of 35wt% H₂O₂ and 106.2g CH₃COOH in the presence of TiO₂ as catalyst. The solution was heated for 2 hours using a magnetic hot plate and stirrer. The product (DLBF) was washed and filtered before being dried in the oven for two hours at 70°C. Finally, the DLBF was immersed into a 6wt% NaOH. The mixture was stirred for 8 hours while being heated to 80°C for 2 hours to dissolve pectin and hemicelluloses. The solution was again filtered. This step was repeated twice or thrice to yield white, soft bamboo cellulose (BC) fiber clumps. The cellulose was oven-dried at 105°C for more than 4 hours before dissolution.

In order to prepare regenerated cellulose film, 5wt% (0.025g) of cellulose was dispersed in 5g ILs, [AMIM]Cl and [BMIM]Cl respectively. The mixture was heated to 90°C under magnetic stirring until cellulose dissolves completely in ILs. The resulting clear, transparent solution was casted on a film applicator and then immediately coagulated in water to obtain transparent cellulose gel and was held with running distilled water to wash the residual ionic liquid after dissolution. The cellulose gel was then vacuum dried at 60°C for 24 hours to yield cellulose films. All films were stored in a conditioning cabinet at 50% relative humidity (RH) and 25°C to ensure the stability of the water content before characterization.

2.1 Particle Size Analyzer (PSA)

The size and distribution of the particles that make up the extracted cellulose was determined analytically using a PSA. By measuring the intensity of light scattered when a laser beam travels through the dispersed particulate cellulose sample, the Mastersizer 3000 employed the concept of laser diffraction to determine the particle size and particle size distribution of cellulose. The size of the particles responsible for the scattering pattern was then determined by analyzing the data acquired [2].

2.2 Fourier-transform infrared spectroscopy (FTIR)

Fourier-transform infrared spectroscopy (FTIR) was used to study the changes in the chemical structure of the cellulose obtained. The FTIR spectra were obtained using an ATR-FTIR spectrometer with transmittance range of the scan was from 4000 to 400cm⁻¹[3].

2.3 X-ray diffraction (XRD)

X-ray diffraction (XRD) was used to study the molecular structural information of the material by determining the degree of crystallinity and crystallite size of the sample. XRD angle for the cellulose was observed by using a PW3040X-ray diffractometer. 2g sample is monitored with a scanning speed of 2°/min at an angle of 10° and 40° by using Cu K α radiation with 40 kV of voltage and 30mA of current [4]. The crystallinity index % (CrI %) of the sample is calculated using the Eq. 1.

$$CrI(\%) = \frac{I_{002} - I_{am}}{I_{002}} \times 100\% \quad Eq. 1$$

I_{002} = peak intensity of the (002) lattice plane

I_{am} = peak intensity of diffraction of amorphous region of cellulose

2.3 Thermogravimetric Analysis (TGA)

The degradation temperature of the bamboo cellulose and films was determined via TGA analysis. The test involved heating 10-20mg of sample from ambient temperature to 600°C under an inert environment of N₂ with 20mL/min flowrate 600°C [5].

2.4 Differential Scanning Calorimetry (DSC)

The difference between the amount of heat needed to raise the temperature of a sample and a reference as a function of temperature was determined using DSC analysis [6]. The melting temperature and degree of crystallinity of the bamboo cellulose and regenerated film were determined via PerkinElmer Diamond DSC where 2mg of sample will be heated from room temperature to 400°C. The analysis was operated at the heating rate of 10°C/min under an inert atmosphere of N₂ with 20mL/min flowrate [7].

3. Results and Discussion

3.1 The Effect of Mechanical Treatment on the Size Distribution of Bamboo Fiber (BF)

The particle size distribution graph in Figure 3.1 suggests monomodal for both samples where both frequency distribution has only one maximum. The volume moment mean, D_v (De Brouckere Mean Diameter) is significant to reflect the particle size that make up the majority of the sample volume. In addition, it emphasizes the presence of large particulates in the sample volume [8]. The results suggest that RBF is mainly consisting of particles of 224µm while sieved BF is of 52.1µm. Clearly, the disintegration of particles is markedly improved after sieving using a 75µm mesh size sieve compared to unsieved raw BF with ball milling alone. The mean size, D_v(10) of RBF is 43.9µm whereas the particles of sieved BF have an average size of 18.1µm, suggesting that the particles mean size have reduced significantly after sieving.

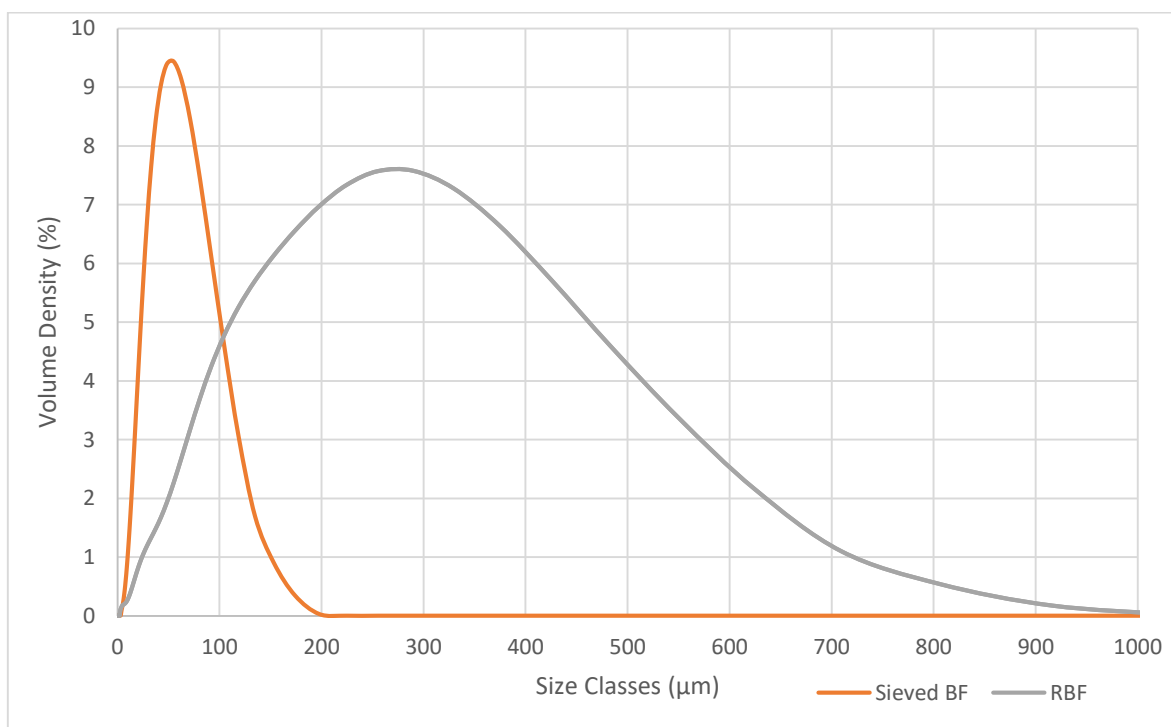


Figure 3.1: Particle size distribution of (a)sieved BF and (b)RBF

3.2 The Effect of Chemical Treatment on The Chemical Composition of Raw Bamboo Fiber (RBF), Delignified Bamboo Fiber (DLBF) and Bamboo Cellulose (BC)

3.2.1 Fourier-transform Infrared Spectroscopy (FTIR)

Figure 3.2 shows the FTIR spectroscopy of RBF, DLBF and BC.

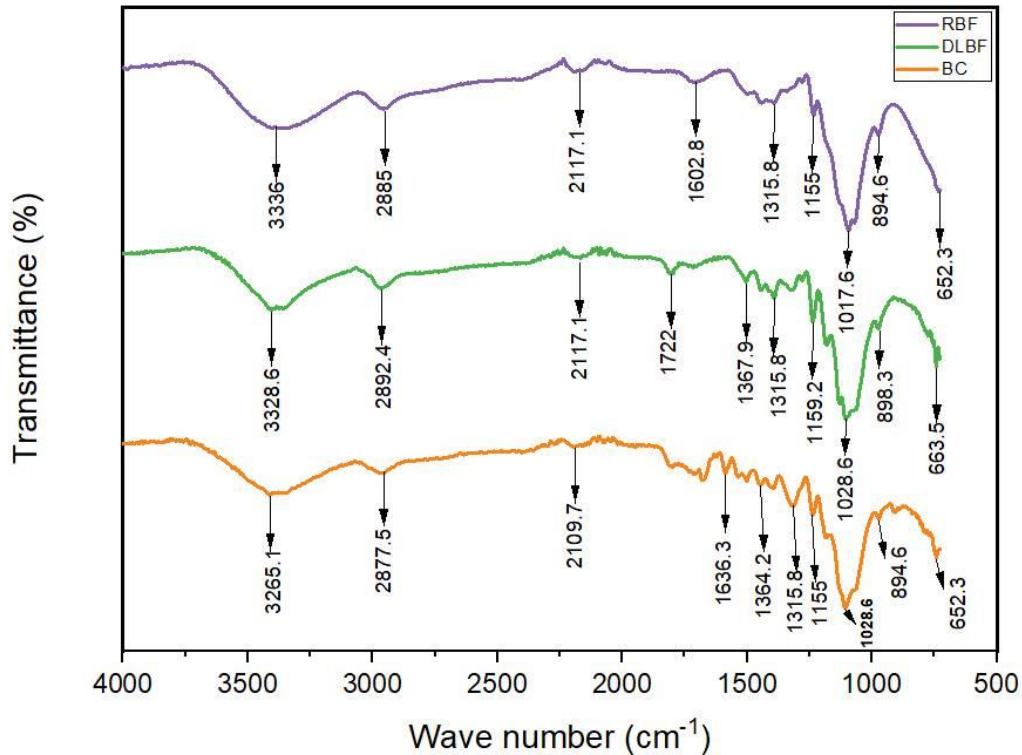
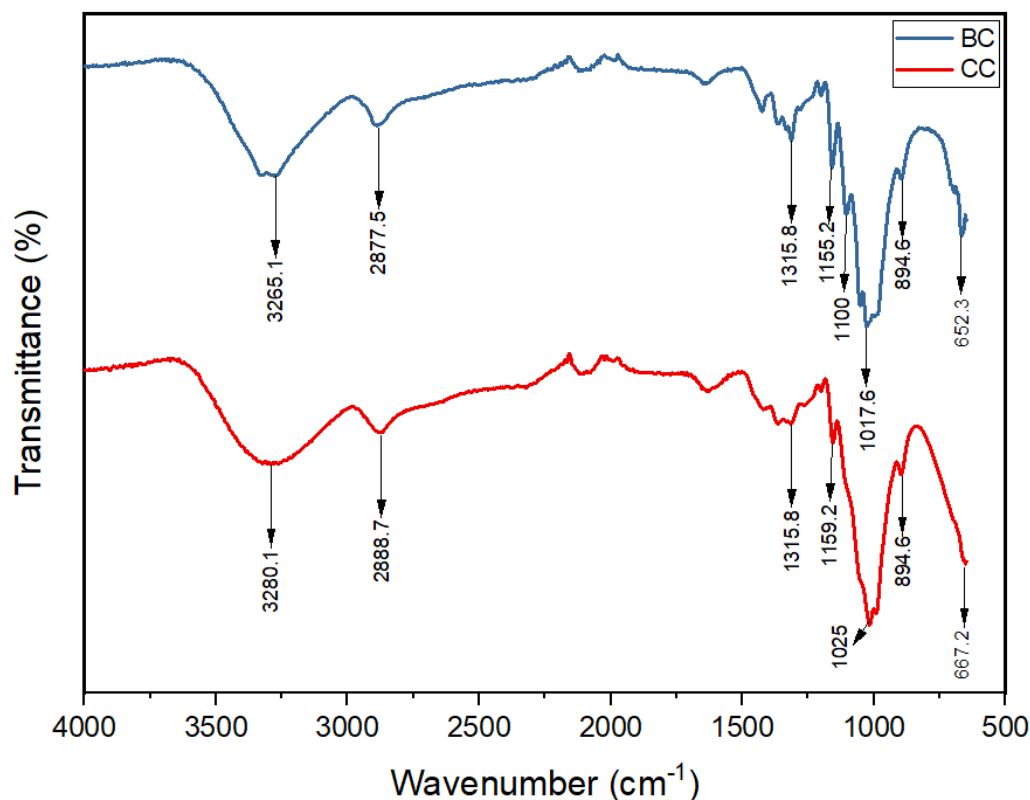


Figure 3.2: FTIR spectra of (a)RBF, (b)DLBF and (c)BC

The composition changed in bamboo fiber was investigated by FTIR spectroscopy to identify the extracted compound after two stages of chemical treatment. Figure 4.2 shows the FTIR spectroscopy RBF, DLBF and BC. The C=C stretching vibration in the aromatic ring of lignin is believed to be responsible for the RBF peak intensity at 1602.8 cm^{-1} [9][10]. Nevertheless, BC did not exhibit C=C stretching in that region, indicating that lignin had been effectively eliminated by the chemical process. The peak intensity band at 3265.1 cm^{-1} of BC is attributed to O-H stretching vibration [9]. The bands at 2877.5 and 1364.2 cm^{-1} are characteristics of C-H stretching and $-\text{CH}_2$ bending, respectively. The peaks at 1636.3 and 894.6 cm^{-1} are attributed to the H-O-H stretching vibration of absorbed water in carbohydrate and the $\text{C}_1\text{-H}$ deformation vibrations of cellulose, respectively [9].

Moving from RBF to DLBF, there is not much change in the chemical composition but there is an obvious change in the intensity peak of 1722 cm^{-1} which is contributed by the presence of C=O stretching frequency of ester linkage of carboxylic group of ferulic and p-coumaric acids in hemicelluloses. The absence of this peak in BC is attributed to the removal of the hemicellulose during the alkaline pre-treatment process [11]. This fact also indicates that hemicelluloses and lignin are removed during the chemical process and the original molecular structure of cellulose is maintained after the matrix components are removed.

The peak at 894.6 cm^{-1} in BC is connected with glycosidic $\text{-C}_1\text{-H}$ deformation, a ring vibration, and $-\text{O-H}$ bending. These characters imply the β -glycosidic linkages between the anhydroglucose units in cellulose [12]. The rise of intensity peak at 1017.6 cm^{-1} confirms that the cellulose content increased due to the alkaline treatment.



Further analysis was made for comparison between commercial cellulose (CC) and bamboo cellulose (BC) as shown in Figure 3.3. It was found that both celluloses have identical peaks. Bands at 3280.1cm^{-1} of CC is related to hydroxyl groups stretching which is identical to peak at 3265.1cm^{-1} of BC. The absorption band at 1315.8cm^{-1} and 2877.7cm^{-1} of BC are contributed by the stretching and deformation vibrations of C-H group in glucose unit. The β -glycosidic linkages between the glucose units in cellulose is responsible for the peak intensity at 894.6cm^{-1} . The bands at 1025cm^{-1} are characteristics of -C-O group of secondary alcohols and ethers functions existing in the cellulose chain backbone which is identical to peak at 1017.6cm^{-1} of BC [13]. Based on the spectrums compared, it can be confirmed that bamboo cellulose obtained is identical to commercial cellulose.

Figure 3.3: FTIR Spectra of (a)CC and (b)BC

3.3 The Effect of Chemical Treatment on the Crystallinity of Bamboo Cellulose

The crystallinity indices of cellulose extracted from bamboo were analysed by XRD. Figure 3.4 shows the X-ray diffractograms patterns of RBF and BC. Cellulose consists mainly of crystalline and amorphous regions formed by intra- or intermolecular hydrogen bonding and van der Waals forces of interactions.

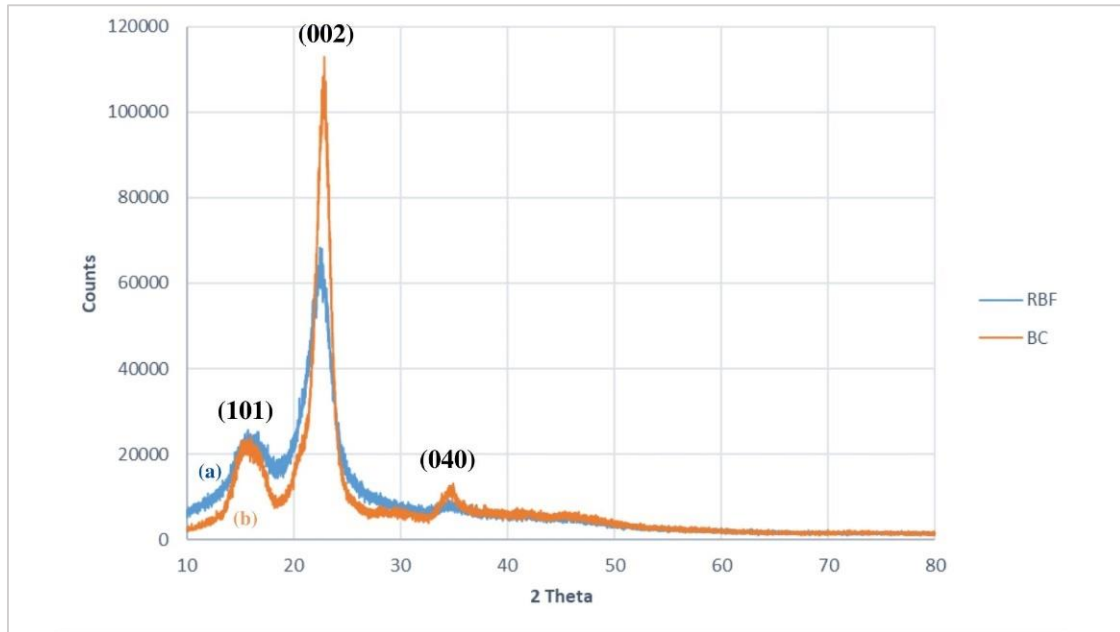


Figure 3.4: X-ray diffractograms patterns of (a)RBF and (b)BC

The lattice planes (040), (002), and (101) of RBF and BC were represented by three typical characteristic peaks of cellulose, with values of $2\theta = 15.05^\circ$, 22.02° and 34.56° , respectively for RBF and 15.94° , 22.92° and 34.45° , respectively for BC. A similar finding was reported by Trilokesh et al., who investigated on cellulose isolated from jackfruit peel and the peaks were recorded at $2\theta = 15.7^\circ$, 22.6° , and 35.19° corresponding to the lattice plane of 040, 002 and 101 [14]. In fact, lattice planes (040) and (002) reflects the crystalline structure. The peak reflecting the crystal zone width was (002), and that reflecting the zone length was (040). The widened peaks shown by RBF suggest the crystalline disorder. On the other hand, the sharper and stronger peaks demonstrated by BC indicate that the amorphous region of lignin and hemicellulose was removed during the chemical treatment.

In addition, the crystalline structure of the cellulose in both samples was not destroyed by both the mechanical and chemical treatments, but its crystallinity was changed. In fact, lattice planes (040) and (002) reflects the crystalline structure. Among them, the peak reflecting the crystal zone width was (002), and that reflecting the zone length was (040).

Both samples feature a typical cellulose type I crystal structure [15]. The most prevalent form of cellulose I is found mostly in the cell walls of plants. There are two different allomorphs of cellulose I (Ia and Ib). In contrast to cellulose Ib, which has a monoclinic unit cell, cellulose Ia has a triclinic unit cell. The majority of cellulose produced from higher plants is Ib, while bamboo cellulose is thought to be almost entirely Ib [16]. It can be highlighted that the crystalline structure of the cellulose in both samples was not destroyed by mechanical and chemical treatments, but the crystallinity index (CrI %) was changed. The crystallinity of both samples is demonstrated by crystallinity index (CrI %), a quantitative indicator of crystallinity [17]. The CrI % of RBF and BC are calculated using Eq 1 and is tabulated in Table 3.1. The degree of crystallinity of RBF was found to be 65.53% whereas 78.17% for BC. It was found that the crystallinity of BC is 16.08% higher than that of RBF. This proves that the chemical treatment process had played an important role in the removal of amorphous components in RBF, which in turn rearranging the cellulose crystalline domains into a more ordered structure, contributing to the increase in the CrI% [18].

Table 3.1: Crystallinity index (CrI %) of RBF and BC

Samples	2θ (Amorphous) (°)		2θ (Crystalline) (°)		Crystallinity Index (CrI %)
	Degree	Intensity (I _{am})	Degree	Intensity (I ₀₀₂)	
RBF	15.05	20420.4	22.02	59241.0	65.53
BC	15.94	22640.0	22.92	103729.0	78.17

3.4 The Effect of Chemical Treatment on The Thermal Properties of Bamboo Cellulose and Regenerated Cellulose Film

The thermal properties of RBF, BC and CC are assessed via TGA and DSC. Although both instruments are used to study the thermal properties of a material, but they work differently and provide different results. In TGA, the weight loss of the sample is measured with the increasing of temperature [19]. DSC, on the other hand, measure the heat flow in and out from the sample due to the temperature difference built up between the sample and a reference [6].

3.4.1 Thermogravimetric Analysis (TGA) of Bamboo Cellulose and Regenerated Cellulose Film from [BMIM]Cl

The thermal analysis of RBF, BC, CC and CCB 1 was performed from ambient temperature to 600°C at 10°C /min and the TGA and DTG thermograms are shown in Figure 3.5 and 3.6.

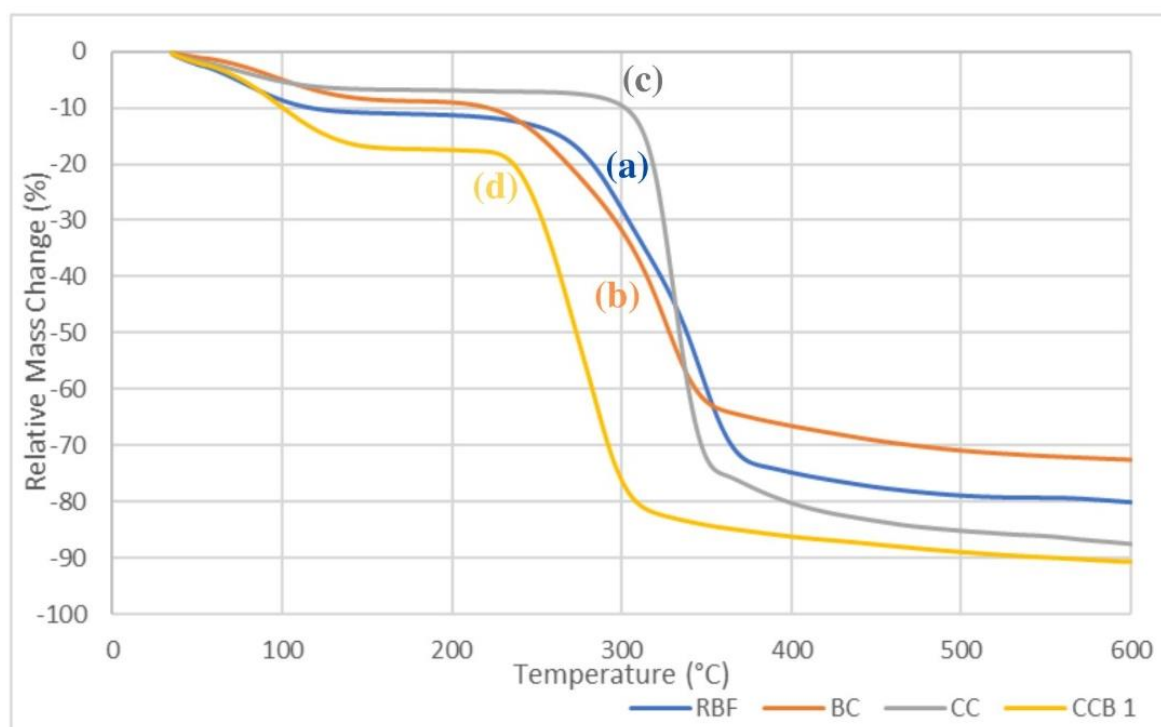


Figure 3.5: TGA result of (a)RBF, (b)BC, (c)CC and (d)CCB 1

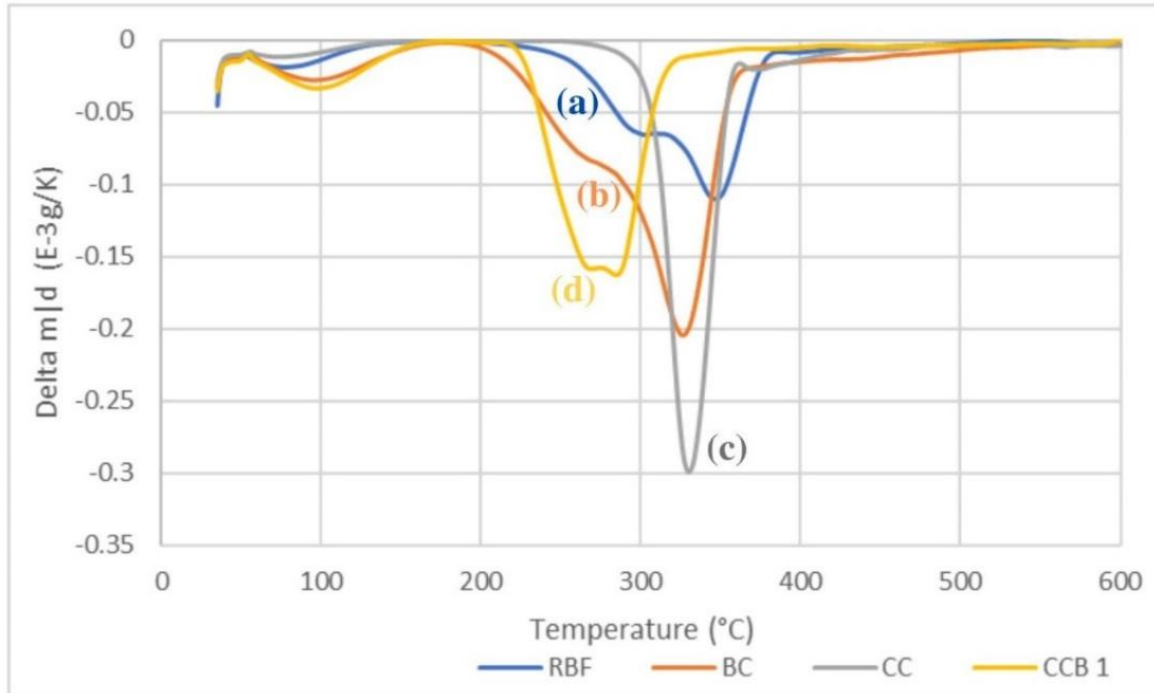


Figure 3.6: DTG result of (a)RBF, (b)BC, (c)CC and (d)CCB 1

As shown in Figure 3.5 and 3.6, all samples exhibit two decomposition stages, corresponding to the slow pyrolysis and fast pyrolysis stage, showing that all samples experience mass loss in two stages. The mass loss of the samples at the slow pyrolysis stage happened around 100°C was due to the volatilization and vaporization of water [8][20]. The mass lost for all samples was in the range of 4%-10% of their total mass, with CCB 1 and BC had the highest and lowest mass loss, respectively. Since all samples were hydrophilic, thus dehydration happened. RBF showing the greatest drop, when compared to BC and CC, suggesting that it contained the most amorphous region due to the presence of both lignin and hemicellulose that is responsible for moisture absorption [21]. This is also supported by the XRD results in 3.3.1 that demonstrated the lower crystallinity of RBF when compared to BC. It is worth nothing that BC and CCB 1 showed continuous weight loss from 100°C to 150°C which was believed to be contributed by the lower intermolecular forces and hydrogen bonding after the mercerization and regeneration process respectively.

Fast pyrolysis, on the other hand, occurred at 220°C-347°C and the weight loss was relatively fast, corresponding to the thermal decomposition of a significant amount of hemicellulose (RBF, BC and CCB 1) which is reflected in the DTG curves. The DTG curves suggest two distinct peaks for RBF, BC and CCB 1 within the range of 250°C -290°C for the first peak, and 325°C-347°C for the latter. Only one peak was observed in the case of CC due to the absence of hemicellulose in CC.

RBF, BC, CC and CCB 1 showed a maximum peak at 346.9°C, 325.8°C, 329.8°C and 285°C respectively, indicating the degradation of cellulose. It was noted that the regenerated cellulose film, CCB 1 had the lowest thermal stability as its degradation temperature was the lowest, 285°C, which was probably caused by the dissolution process. This results also suggested that the thermal stability of the samples increased in the following order:

$$\text{CCB 1} < \text{BC} < \text{CC} < \text{RBF}$$

The low thermal stability of CCB 1 was due to the disruption of the inter- and intra-molecular hydrogen bonds of CC during the dissolution process in [BMIM]Cl [21]. At the same time, it was noted that BC had lower thermal stabilities than RBF and CC as most of the hydrogen bonds and the cellulose molecular chains were degraded by NaOH during mercerization. According to Shen et al. (2009), the cellulose (cleavage of 1,4-glycosidic bond) was decomposed to form a smaller fragment, which is

known as levedglucosan (1.6-anhydrous- β -D-glucopyranose) [22]. RBF, in contrast showed the highest degradation temperature suggested the presence of lignin. Lignin is difficult to degrade owing to its complex structure. The interaction of lignin with the cellulose will prevent the degradation of cellulose thus showing a higher temperature [23].

The thermogram of bamboo is parallel to the findings from Yang et al. (2006) have demonstrated that hemicellulose, cellulose, and lignin breakdown took place at temperatures between 220°C and 300°C, 300°C and 340°C, and above 340°C, respectively [24]. In addition, Yang et al. (2006) highlighted that the degradation of these components take place in the following steps: (1) loss of moisture, (2) polymer decomposition begins with hemicellulose component, (3) cellulose and lignin contribute to weight loss after hemicellulose has decomposed, (4) most rapid rate of decomposition contributed by cellulose and lignin, and (5) the remaining lignin continues to decompose above 340 °C. The literature studies by Pang et al. (2014) showed similar results with this research, where the thermal stabilities regenerated cellulose films were lower than that of original cellulose, which was claimed to be contributed by the lower crystallinity of regenerated cellulose [25].

Hemicellulose is a heterogeneous polymeric network with an amorphous structure and has lower molecular weight than cellulose [26]. This eventually results in low thermal stability of hemicellulose which can be easily removed and decomposed to volatile compound such as carbon dioxide, carbon monoxide and some hydrocarbons at temperature range from 220°C and 300°C [24]. Lignin, on the other hand is full of aromatic ring, high branched and form linkage by various chemical bonds subsequently contributes to a wide range of thermal degradation temperature [27]. To illustrate this, the DTG curve of RBF showed a longer range compared to BC and CC due to presence of lignin and hemicellulose.

The percentage weight residue for CCB 1 is 9%, CC is 12%, 20% for BC and 27% for RBF. Higher weight residue was showed by RBF probably due to the impurities as compared to BC.

3.4.2 Differential Scanning Calorimetry (DSC) of Bamboo Cellulose and Regenerated Cellulose Film from [BMIM]Cl

DSC is used to study the thermal absorption of the sample. A negative curve indicates an endothermic reaction where a positive curve, on the other hand indicates an exothermic reaction. An endothermic reaction is caused by the melting or evaporation of the sample while an exothermic reaction is caused by the decomposition of the sample as heat release when the sample decomposes to volatile substances. When compared to endothermic reactions, which depict melting, phase transitions, evaporation, dehydration, and pyrolysis, exothermic reactions offer insights about the sample's crystallization, oxidation, combustion, decomposition, and chemical processes [3]. Figure 3.7 shows the DSC results of RBF, BC, CC and CCB 1.

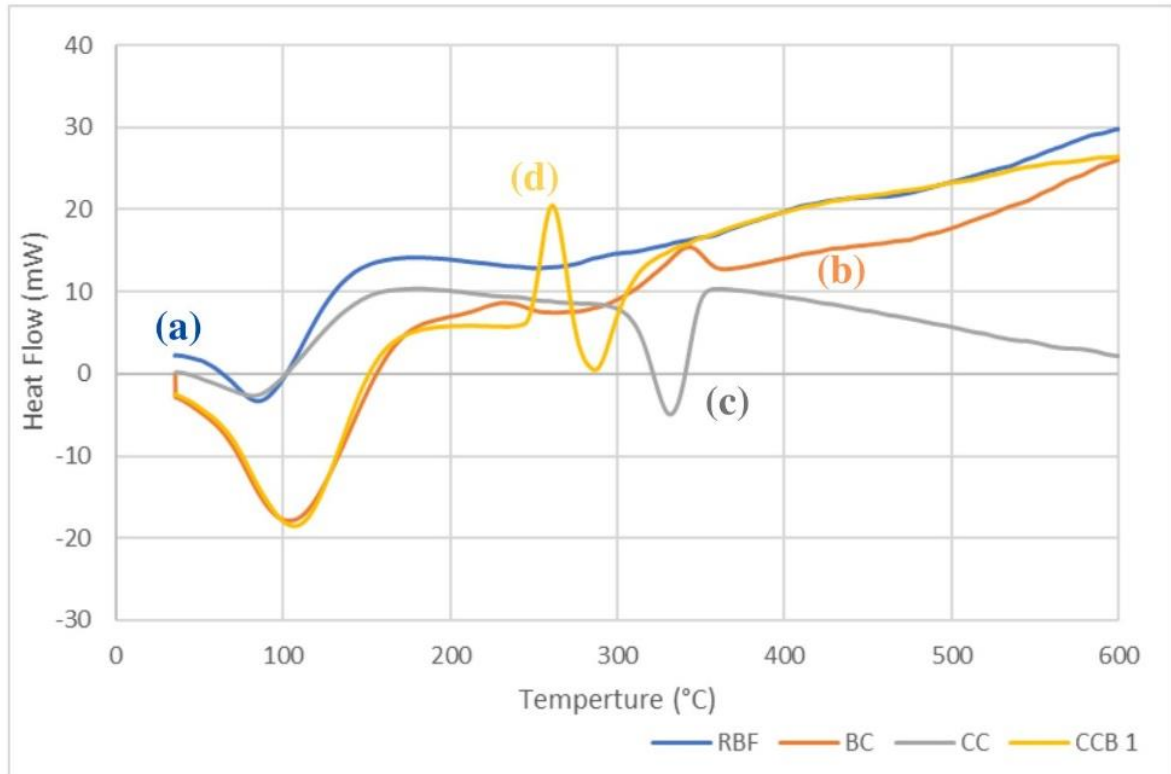


Figure 3.7: DSC result of (a)RBF, (b)BC, (c)CC and (d)CCB 1

The first endothermic curve occurred below 120°C for all the samples, suggesting the evaporation of water which is also shown in the TGA studies (slow pyrolysis), which is thought to correlate with the presence of amorphous component. It is noted that CCB 1 showed the highest glass transition temperature, T_g 107.9°C which was probably caused by disruption of the inter- and intramolecular hydrogen bonds of CC during the dissolution of cellulose in [BMIM]Cl. RBF showed a wider exothermic curve which occurred from 240°C to 380°C which matches the thermal decomposition TGA results. RBF is composed of three major components, lignin, hemicellulose and cellulose which explained the wide degradation temperature showed. The first exothermic hump in the DSC curve for RBF is about 290°C which is due to the thermal degradation of hemicellulose and the glycosidic linkages of cellulose which is aligned with its TGA results. According to Ball et al. (2004), the exothermic peak could be caused by the charring process which is caused by lignin and hemicellulose [28]. BC also showed a narrower exothermic curve as compared to RBF as lignin and hemicellulose were removed during chemical pre-treatment.

The second endotherm transition of CC and could be seen at near 330°C, corresponding to the maximum of DTG peak, showing the decomposition of cellulose. The weight loss of CC showed in its TGA curve supported this finding too. This endotherm was associated to the melting of cellulose caused the breakage of glycosidic bonds and the depolymerization of cellulose. This finding is in agreement with Yeng's et al. (2005) work who observed an endotherm transition of cellulose at 319.67°C. BC, on the other hand exhibited an exothermic curve from 240°C to 360°C where a sharp peak was observed at 350°C, contributing to the decomposition of cellulose [19].

Moving to CCB 1, it showed a lower endothermic transition temperature at around 290°C as compared to CC. The lower transition temperature was contributed by the breakdown of intra- and intermolecular hydrogen bonds during dissolution and regeneration process, which leads to a decrease in crystallinity. This finding could be further supported by the low thermal stability of CCB 1 as discussed in 3.4.1. A similar finding was reported by Yeng et al. [19].

3.5 Dissolution Effect of Bamboo Cellulose in Ionic Liquids

The dissolution effect of bamboo cellulose in both [AMIM]Cl and [BMIM]Cl at 90°C are discussed in this section and the results are tabulated in Table 3.2. It was found that at 90°C, CC (5wt%) forms film flakes instead of a uniform piece of film after coagulated with water as shown in Figure 3.8. The film appears to be fragile when it was touched.

Under the same condition using 5wt% BC, powder was observed (Figure 3.9) when the solution is coagulated with water. The powder was believed to be the cellulose, suggesting incomplete cellulose dissolution. The remaining cellulose-IL solution samples after dissolution were dissolved in water (Figure 3.10). The reappearing of cellulose powder and the inability to form regenerated cellulose films were believed to be contributed by the poor dissolution rate of cellulose in ILs. Several contributing factors were discussed by the researcher in the next section, 3.6.

Table 3.2: Cellulose Dissolution in ILs at 90°C

Cellulose sample Dissolution with ILs [AMIM]Cl at 90°C		Film formation	Description
[AMIM]Cl	CCA 1 (5wt%)	NO	dissolves in water
	CCA 2 (4wt%)	NO	dissolves in water
	BCA 1 (5wt%)	NO	dissolves in water
	BCA 2 (4wt%)	NO	dissolves in water
[BMIM]Cl	CCB 1 (5wt%)	YES	flakes film
	CCB 2 (4wt%)	NO	dissolves in water
	CCB 3 (2wt%)	NO	dissolves in water
Table 3.2 (Continued)			
	BCB 1 (5wt%)	NO	Obtain powder
	BCB 2 (4wt%)	NO	dissolves in water

*CC: commercial cellulose

BC: bamboo cellulose

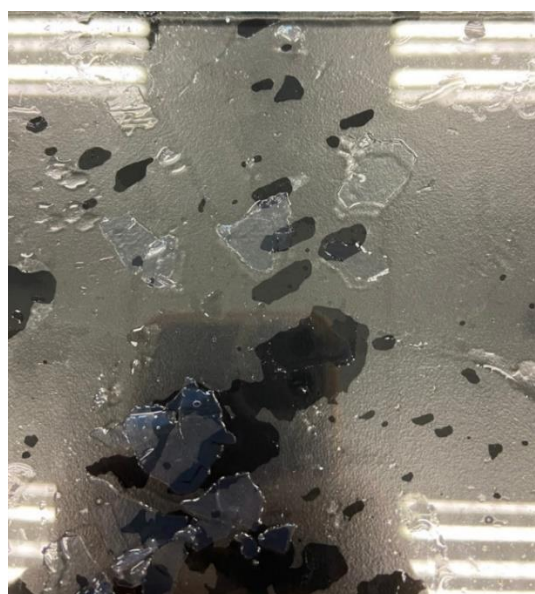


Figure 3.8: Film flakes



Figure 3.9: Powder



Figure 3.10: Cellulose-ILs solution dissolve in water

3.6 Contributing Factors to Regenerated Bamboo Cellulose Film Failure

3.6.1 The Absence of Cosolvent

Ionic liquids are often very viscous, and it is known that adding a polymer, in this case, cellulose to it can make it even more viscous. Because of this, the dissolution of high amounts of cellulose in an ionic liquid can be limited not only by unfavourable solute-solvent interactions but also by mass transport [29]. ILs have been shown to significantly enhance cellulose dissolution when co-solvents that are highly polar and aprotic are added. For instance, dimethyl sulfoxide, also known as DMSO which is a highly polar aprotic organic liquid, having high and good thermal stability appears to be a

good solvent [30]. In fact, the addition of DMSO as a co-solvent was found to induce an exponential decrease in the viscosity of cellulose-ionic liquid solution, accelerating mass transfer and thus, lowering the temperature required for cellulose dissolution without affecting the interactions between cations and anions or between ILs and cellulose [31][32]. Additionally, the adding of co-solvents was proved to decrease the internal frictional force of ILs and the binding force of cellulose, thus lowering its viscosity [33]. According to some researchers, the presence of cosolvents causes ILs to separate into solvated cations and release anions, increasing the interactions between anions and cellulose, thus facilitating dissolving [34].

In this context, the results suggest that [AMIM]Cl is more viscous than [BMIM]Cl as cellulose-[AMIM]Cl solutions dissolves in water, instead of coagulate to form film. To illustrate this, 5wt% CC in [BMIM]Cl forms flakes film, yet under the same circumstances using [AMIM]Cl, no film was observed. Similarly, when using 5 wt% BC, powder was seen in the case of [BMIM]Cl after coagulated with water the solution was dissolved in water in the case of [AMIM]Cl. Additionally, it is believed that by adding co-solvents, for example DMSO, the viscosity of the cellulose-ILs can be significantly reduced to enhance the rate of dissolution, thus forming uniform films.

3.6.2 Heating Method

Microwave heating has been proven to be an alternative to conventional heating approach and has been successfully employed in organic and inorganic synthesis and carbohydrate breakdown owing to its thermal and non-thermal effects, the ability to accelerate collisions between ions and molecules and the rapid rotation of dipoles [35][36]. Additionally, the issue of heat transfer resistance can be resolved as microwave radiation can rapidly penetrate into particles to obtain more uniform and efficient heating. Therefore, it stands to reason to believe that cellulose might be quickly dissolved in ILs employing ultrasonic and microwave heating [35]. In the studies of Zhang et al. (2017), microwave-assisted dissolution, and sonication-assisted dissolution were all discovered to considerably speed up the disintegration of cellulose [31]. According to Swatloski et al. (2002), heating in a microwave oven can significantly enhance the substrate's dissolving rates [37]. In addition, microwave heating was demonstrated by Pinkert et al. (2009) to be an internal heating process as a result of polar molecules directly absorbing energy. As a result, the H-bond network is more effectively broken down, leading to rapid depolymerization of biopolymers. The combination of cellulose and ILs has been proven to have the ability to effectively absorb microwave radiation and transform it into heat [38].

In this research, all cellulose-ILs solutions were heated using a magnetic hot plate with stirrer during the dissolution process which has contributed to poor dissolution rate as suggested from the findings. This stirring method certainly provides uniform heating, however, internal heating process to effectively break down the H-bond network of cellulose which will lead to the disintegration of cellulose could not be achieved.

3.6.3 Degradation of Cellulose

Cellulose can degrade to produce oligosaccharide or even monosaccharide which could hardly be recovered when dissolved in ILs especially at high temperature ($\geq 130^\circ\text{C}$) for prolonged period of time (≥ 8 h) [35][39]. The performance of cellulose membrane and aerogel prepared with ILs is compromised by cellulose degradation, which also impacts the quality of spinning fibres. It was challenging to create cellulose products if the cellulose was excessively degraded [39]. In order to prevent cellulose degradation, lowering temperature and dissolution time were taken into consideration. Unfortunately, these approaches will reduce the efficiency of cellulose dissolution, thus limiting the use of ILs in the cellulose sector. Yang et al. (2019) suggested that adding an additive to inhibit cellulose degradation. He added that the additive is more likely to form H bonds with the three ipsilateral hydroxyls of cellulose than BMIMCl, and the remaining hydroxyl groups of cellulose can react with ILs to ensure cellulose dissolution. As known, intermolecular hydrogen bonds can be easily formed between the acidic group ($-\text{SO}_3\text{H}$, $-\text{COOH}$) and basic group ($-\text{NH}_2$). Thus, in Yang et al. (2019) studies, amino acids with a carboxyl group, $-\text{COOH}$ and an amino group, $-\text{NH}_2$ were proposed as an additive to inhibit the degradation of cellulose [39].

4. Conclusion

In this research project, nature cellulose was successfully extracted from raw bamboo, *Schizostachyum grande* through a combination of mechanical and chemical treatment. The researcher believed that the absence of co-solvent, conventional heating of cellulose-IL and degradation of cellulose during dissolution have contributed to partial successful of the film formation. The bamboo cellulose, raw bamboo fiber, commercial cellulose and regenerated cellulose film had subjected to PSA, FTIR, TGA, XRD and DSC in order to study the changes of their sizes, chemical composition, thermal stability as well as their crystallinity. Based on the experimental data, the particle size of the raw bamboo fibre significantly decreased after sieving through a 75 μm mesh size sieve. The extraction of bamboo cellulose has been successfully synthesized using a combination of mechanical and chemical treatment. The FTIR results suggest an obvious disappearance of 1722 cm^{-1} and 1602.8 cm^{-1} , indicating that C=O stretching frequency of ester group and the stretching vibration of aromatic rings caused but lignin was successfully removed. In addition, when compared to commercial cellulose, the extracted cellulose shows identical peaks. The crystallinity of extracted bamboo cellulose is found to increase as high as 16.08% higher when compared to the raw bamboo fiber due to the removal of lignin and hemicellulose which are amorphous in nature. The regenerated cellulose film formed in [BMIM]Cl had the lowest thermal stability which was probably caused by the dissolution and regeneration process which has disrupted inter- and intra-molecular hydrogen bonds of cellulose. The thermal stability of bamboo cellulose is lower than raw bamboo fiber and commercial cellulose as most of the hydrogen bonds and the cellulose molecular chains were degraded by NaOH during mercerization. The absence of co-solvent, conventional heating and degradation of cellulose into oligosaccharide or even monosaccharide have believed to significantly affect the dissolution of cellulose, which in turns contribute to the partial successful of film formation.

Acknowledgement

The author would also like to thank the Faculty of Engineering Technology, Universiti Tun Hussein Onn Malaysia for its support.

References

- [1] Abdoulhdi, A. B. O., Abdulrahman, A. B. A. M., Sapuan, S. M., Ilyas, R. A., Asyraf, M. R. M., Rahimian, K. S. S., & Petru, M. (2021). Micro-and Nanocellulose in Polymer Composite Materials: A Review. *Polymers*, 13, 231.
- [2] Abdulkarim, M., Grema, H. M., Adamu, I. H., Mueller, D., Schulz, M., Ulbrich, M., ... & Preusser, F. (2021). Effect of Using Different Chemical Dispersing Agents in Grain Size Analyses of Fluvial Sediments via Laser Diffraction Spectrometry. *Methods and protocols*, 4(3), 44.
- [3] Naim, A., Soo Yun Tan, C., & Liew, F. K. (2022). Thermal Properties of Bamboo Cellulose Isolated from Bamboo Culms and Shoots. *BioResources*, 17(3).
- [4] Huang, Z., Liu, C., Feng, X., Wu, M., Tang, Y., & Li, B. (2020). Effect of regeneration solvent on the characteristics of regenerated cellulose from lithium bromide trihydrate molten salt. *Cellulose*, 27, 9243-9256.
- [5] Díez, D., Urueña, A., Piñero, R., Barrio, A., & Tamminen, T. (2020). Determination of hemicellulose, cellulose, and lignin content in different types of biomasses by thermogravimetric analysis and pseudocomponent kinetic model (TGA-PKM method). *Processes*, 8(9), 1048.
- [6] Picó, Y. (Ed.). (2012). *Chemical analysis of food: Techniques and applications*. Academic Press.
- [7] Kim, J. W., Park, S., Harper, D. P., & Rials, T. G. (2013). Structure and thermomechanical properties of stretched cellulose films. *Journal of applied polymer science*, 128(1), 181-187.

- [8] Hlobil, M., Kumpová, I., & Hlobilová, A. (2022). Surface area and size distribution of cement particles in hydrating paste as indicators for the conceptualization of a cement paste representative volume element. *Cement and Concrete Composites*, 134, 104798.
- [9] Liew, F. K., Hamdan, S., Rahman, M., Rusop, M., Lai, J. C. H., & Hossen, M. (2015). Synthesis and characterization of cellulose from green bamboo by chemical treatment with mechanical process. *Journal of Chemistry*, 2015.
- [10] Rosa, S. M., Rehman, N., de Miranda, M. I. G., Nachtigall, S. M., & Bica, C. I. (2012). Chlorine-free extraction of cellulose from rice husk and whisker isolation. *Carbohydrate Polymers*, 87(2), 1131-1138.
- [11] Chen, W., Yu, H., Liu, Y., Hai, Y., Zhang, M., & Chen, P. (2011). Isolation and characterization of cellulose nanofibers from four plant cellulose fibers using a chemical-ultrasonic process. *Cellulose*, 18(2), 433-442
- [12] Nguyen, H. D., Mai, T. T. T., Nguyen, N. B., Dang, T. D., Le, M. L. P., & Dang, T. T. (2013). A novel method for preparing microfibrillated cellulose from bamboo fibers. *Advances in Natural Sciences: Nanoscience and Nanotechnology*, 4(1), 015016.
- [13] Abderrahim, B., Abderrahman, E., Mohamed, A., Fatima, T., Abdesselam, T., & Krim, O. (2015). Kinetic thermal degradation of cellulose, polybutylene succinate and a green composite: comparative study. *World J. Environ. Eng*, 3(4), 95-110.
- [14] Trilokesh, C., & Uppuluri, K. B. (2019). Isolation and characterization of cellulose nanocrystals from jackfruit peel. *Scientific Reports*, 9(1), 1-8.
- [15] Yu, H., Gui, C., Ji, Y., Li, X., Rao, F., Huan, W., & Li, L. (2022). Changes in Chemical and Thermal Properties of Bamboo after Delignification Treatment. *Polymers*, 14(13), 2573.
- [16] Gündüz Ergün, B., & Çalık, P. (2016). Lignocellulose degrading extremozymes produced by *Pichia pastoris*: current status and future prospects. *Bioprocess and Biosystems Engineering*, 39, 1-36.
- [17] Sa, Y., Guo, Y., Feng, X., Wang, M., Li, P., Gao, Y., ... & Jiang, T. (2017). Are different crystallinity-index-calculating methods of hydroxyapatite efficient and consistent? *New Journal of Chemistry*, 41(13), 5723-5731.
- [18] Orrabalis, C., Rodríguez, D., Pampillo, L. G., Londoño-Calderón, C., Trinidad, M., & Martínez-García, R. (2020). Characterization of nanocellulose obtained from *Cereus Forbesii* (a South American cactus). *Materials Research*, 22.
- [19] Rajisha, K. R., Deepa, B., Pothan, L. A., & Thomas, S. (2011). Thermomechanical and spectroscopic characterization of natural fibre composites. *Interface Engineering of Natural Fibre Composites for Maximum Performance*, 241-274.
- [20] Yeng, L. C., Wahit, M. U., & Othman, N. (2015). Thermal and flexural properties of regenerated cellulose (RC)/poly (3-hydroxybutyrate) (PHB) biocomposites. *Jurnal Teknologi*, 75(11).
- [21] Youssefian, S., & Rahbar, N. (2015). Molecular origin of strength and stiffness in bamboo fibrils. *Scientific reports*, 5(1), 1-13.
- [22] Reddy, K. O., Maheswari, C. U., Dhlamini, M. S., Mothudi, B. M., Zhang, J., Zhang, J., ... & Rajulu, A. V. (2017). Preparation and characterization of regenerated cellulose films using borassus fruit fibers and an ionic liquid. *Carbohydrate polymers*, 160, 203-211.
- [23] Shen, D. K., & Gu, S. (2009). The mechanism for thermal decomposition of cellulose and its main products. *Bioresource technology*, 100(24), 6496-6504.
- [24] Brebu, M., & Vasile, C. (2010). Thermal degradation of lignin—a review. *Cellulose Chemistry & Technology*, 44(9), 353.

- [25] Yang, H., Yan, R., Chen, H., Lee, D. H., Liang, D. T., & Zheng, C. (2006). Mechanism of palm oil waste pyrolysis in a packed bed. *Energy & Fuels*, 20(3), 1321-1328.
- [26] Pang, J. H., Liu, X., Wu, M., Wu, Y. Y., Zhang, X. M., & Sun, R. C. (2014). Fabrication and characterization of regenerated cellulose films using different ionic liquids. *Journal of Spectroscopy*, 2014.
- [27] Zakikhani, P., Zahari, R., Sultan, M. T. H., & Majid, D. L. A. A. (2016). Thermal degradation of four bamboo species. *BioResources*, 11(1), 414-425.
- [28] Deng, Y., Zhao, H., Qian, Y., Lü, L., Wang, B., & Qiu, X. (2016). Hollow lignin azo colloids encapsulated avermectin with high anti-photolysis and controlled release performance. *Industrial Crops and Products*, 87, 191-197.
- [29] Pelissari, F. M., Sobral, P. J. D. A., & Menegalli, F. C. (2014). Isolation and characterization of cellulose nanofibers from banana peels. *Cellulose*, 21, 417-432.
- [30] Andanson, Jean-Michel; Bordes, Emilie; Devémy, Julien; Leroux, Fabrice; Pádua, Agílio A. H.; Gomes, Margarida F. Costa (2014). Understanding the role of co-solvents in the dissolution of cellulose in ionic liquids. *Green Chemistry*, 16(5), 2528-. doi:10.1039/C3GC42244E
- [31] Xu, A., Zhang, Y., Zhao, Y., & Wang, J. (2013). Cellulose dissolution at ambient temperature: Role of preferential solvation of cations of ionic liquids by a cosolvent. *Carbohydrate polymers*, 92(1), 540-544.
- [32] Lv, Y., Wu, J., Zhang, J., Niu, Y., Liu, C. Y., He, J., & Zhang, J. (2012). Rheological properties of cellulose/ionic liquid/dimethylsulfoxide (DMSO) solutions. *Polymer*, 53(12), 2524-2531.
- [33] Zhang, J., Wu, J., Yu, J., Zhang, X., He, J., & Zhang, J. (2017). Application of ionic liquids for dissolving cellulose and fabricating cellulose-based materials: state of the art and future trends. *Materials Chemistry Frontiers*, 1(7), 1273-1290.
- [34] Xu, H., Huang, L., Xu, M., Qi, M., Yi, T., Mo, Q., ... & Liu, Y. (2020). Preparation and properties of cellulose-based films regenerated from waste corrugated cardboards using [Amim] Cl/CaCl₂. *ACS omega*, 5(37), 23743-23754.
- [35] Acharya, S., Liyanage, S., Parajuli, P., Rumi, S. S., Shamshina, J. L., & Abidi, N. (2021). Utilization of Cellulose to Its Full Potential: A Review on Cellulose Dissolution, Regeneration, and Applications. *Polymers*, 13(24), 4344.
- [36] Lan, W., Liu, C. F., Yue, F. X., & Sun, R. C. (2013). Rapid dissolution of cellulose in ionic liquid with different methods. *Cellulose Fundamental Aspects*, 179-196.
- [37] Sánchez, P. B., Tsubaki, S., Pádua, A. A., & Wada, Y. (2020). Kinetic analysis of microwave-enhanced cellulose dissolution in ionic solvents. *Physical Chemistry Chemical Physics*, 22(3), 1003-1010.
- [38] Swatloski, R. P., Spear, S. K., Holbrey, J. D., & Rogers, R. D. (2002). Dissolution of cellose with ionic liquids. *Journal of the American chemical society*, 124(18), 4974-4975.
- [39] Yang, J., Lu, X., Yao, X., Li, Y., Yang, Y., Zhou, Q., & Zhang, S. (2019). Inhibiting degradation of cellulose dissolved in ionic liquids via amino acids. *Green Chemistry*, 21(10), 2777-2787.